IOP Conf. Series: Materials Science and Engineering **316** (2018) 012059 doi:10.1088/1757-899X/316/1/012059

CFD investigation of pentamaran ship model with chine hull form on the resistance characteristics

Yanuar[1] **and W Sulistyawati**[2]
[1] Department of Mechanical Engineering, Universitas Indonesia, Depok 16424, Indonesia
[2] Graduate Student Department of Mechanical Engineering, Universitas Indonesia, Depok 16424, Indonesia

E-mail: yanuar@eng.ui.ac.id

Abstract. This paper presents an investigation of pentamaran hull form with chine hull form to the effects of outriggers position, asymmetry, and deadrise angles on the resistance characteristics. The investigation to the resistance characteristics by modelling pentamaran hull form using chine with symmetrical main hull and asymmetric outboard on the variation deadrise angles: 25^o, 30^o, 35^o and Froude number 0,1 to 0,7. On calm water resistance characteristics of six pentamaran models with chine-hull form examined by variation of deadrise angles by using CFD. Comparation with Wigley hull form, the maximum resistance drag reduction of the chine hull form was reduced by 15.81% on deadrise 25^0, 13.8% on deadrise 30^0, and 20.38% on deadrise 35^0. While the smallest value of total resistance coefficient was generated from chine 35^0 at R/L:1/14 and R/L:1/7. Optimum hull form for minimum resistance has been obtained, so it is interesting to continue with angle of entrance and stem angle of hull for further research.

1. Introduction

Many studies established that pentamaran better than monohull, i.e.: large volume and deck, low resistance at high speed, good stability, and good sea keeping performance. The factors affected mutual on multihull were viscosity resistance due to the wide variation of the wetted surface on the changes of pressure and speed, and wave making resistance as effect engagement of the cross section along the ship and spreads of the wave. Outriggers position to the main hull contributed to influence on frictional resistance and stability [1]. The Asymmetric outrigger configuration and separation distance resulted change in resistance and there is no single configuration that consistently outperforms the other configuration across the entire speed range [2]. Frictional resistance on pentamaran increased as a consequence on enhancement of wetted surface area hull form, but wave making resistance can be reduced with a slender hull form. [3] has defined wave making resistance reduction and enhancement of frictional resistance were affected by the hull length to width ratio (L/B).

Minimization resistance of ship there are several ways such as modeling hull form or other ways, e.g.: polymer, microbubbles [4]. Hull form very significant impact on the ship, then modeling with the precise configuration on pentamaran was indispensable. Researches on pentamaran generally use Wigley hull form, this study use chine hull form to investigate and compare with Wigley. The specialty of this chine hull form in some studies shown advantages such as: reducing resistance, easier

and faster in the building process. Experiment [5] shown symmetrical chine hull form on catamarans could reduce wave resistance, interference between hull due to resistance will tend to fall on Fr > 0,5. [6] found that chine more profitable on Fr > 0.75 compared with NPL series, while in sea keeping performance; rounded models are superior in displacement conditions. [7] had compared chine for catamarans and Wigley model by a computer program SHIPFLOW. Wigley hull form in deep waters have a higher value Cw (wave coefficient) at 0.3 < Fr <0.6, and in shallow waters the highest Cw value at Fr 0.4. While the chine hull form, Cw tend to fall at 0.6 <Fr <0.7 in line with the decrease in depth, and the highest value Cw in shallow waters occurred at Fr 0.4.

Ship performance is determined by parameters: L/B, $A_P / V^{2/3}$, LCG, deadrise angle, angle variation along the hull, and shape of chine [8]. [9] had used multihull with chine get hydrodynamics of the catamaran on deadrise angle 0^o-20^o lift coefficient will improve with decreasing spacing of outriggers and high Froude numbers in line increase of deadrise angle. But at larger deadrise angles, high Froude numbers and the gap of outriggers more widen the complex effects occur where the waves flow direction resulting in pressure on the rear area of hull, and also resulted in lift coefficient. [10] were using configuration pentamaran Wigley hull form with numerical method to analyse hydrodynamic characteristics at speed variation. Specifically of this study is investigating the calm-water total resistance, frictional and residuary characteristic of a pentamaran with chine hull form at variation of deadrise angles on 25^0, 30^0, 35^0. The numerical analyses based on computational fluid dynamics (CFD) modelling and validation with last experimental data.

2. Methodology

Experimental and numerical modelling techniques are very important to get hull form with good hydrodynamic, performance and safety. Experimental for multihull ships were first performed by [11] on catamarans to obtain optimal hull with minimum resistance. [12] with numerical computational approach based on [13] determined resistance and motions on catamaran, trimaran, quadrimaran and pentamaran using Wigley hull form on several configurations. He mentioned that the waves making resistance on multihull always the biggest component as the speed or value of Fr increase.

Based on the hypothesis of Froude that the total resistance consists of two components, i.e.: frictional resistance (R_F) and the residuary resistance (R_R).

$$R_T = R_F + R_R \tag{1}$$

The analysis data experiment using ITTC'57 methodology for calculate the total resistance coefficient (C_T):

$$C_T = C_F + C_R \tag{2}$$

$$C_F = \frac{0.075}{(\log Rn - 2)^2} \tag{3}$$

Pentamaran consists of one main hull, two inners and two outers hull, with different Reynold number, then the frictional resistance coefficient calculated by:

$$C_F = C_{Fmain}\frac{S_{main}}{S_T} + C_{F1}\frac{2side_1}{S_T} + C_{F2}\frac{2Side_2}{S_T} \tag{4}$$

Then the residual coefficient was given by:

$$C_R = C_T - C_T \tag{5}$$

2.1. CFD Method

This study was investigation a K-ε model transformed the outer boundary layer and the free stream [14]. In a large variety of different flow, K-ε model has been used successfully. The K-ε model [15] is numerical integrated equation of viscous sub layer used in Computational Fluid Dynamics (CFD) to

simulate characteristics of turbulent flow. It was generally used to mixing-length model, to find algebraically turbulent length scales in high complexity flows. K is turbulent kinetic energy determines in the turbulence, ε. A nonlinear boundary condition on ε allows using of a homogeneous boundary condition.

The mathematical model for free surface flow was based on the homogenous multiphase Eulerian–Eulerian fluid approach. This approach shares the same velocity field and other relevant fields such as temperature, turbulence, etc. Numerical method was derived from Navier Stokes' equations where using a Volume of Fluid (VOF) approach. Incompressible Reynolds averaged Navier-Stokes (RANS) was expressed by [16].

$$\rho\frac{\vartheta U_i}{\vartheta t}+\rho U_j\frac{\vartheta U_i}{\vartheta x_j}=-\frac{\vartheta P}{\vartheta x_i}+\frac{\vartheta T_{ij}}{\vartheta x_j} \quad (6)$$

$$\left(\frac{\vartheta\rho}{\vartheta t}+U_j\frac{\vartheta\rho}{\vartheta x_j}\right)+\rho\frac{\vartheta U}{\vartheta x_i}=0 \quad (7)$$

Equation (6) as momentum equation (second Newtonian law for fluids) and equation (7) as continuity equation. Where, ρ: fluid's density, U_i: velocity components, P: pressure, and T_{ij}: components of viscous stress tensor as follows:

$$T_{ij}=(2\mu S_{ij}-\rho\overline{U_iU_j}) \quad (8)$$

$$S_{ij}=\frac{1}{2}\left(\frac{\vartheta U_i}{\vartheta x_j}+\frac{\vartheta U_j}{\vartheta x_i}\right) \quad (9)$$

where ${}^{\vartheta U_i}/_{\vartheta x_i}=0$ as effect of turbulence on the flow by Reynolds Stress (RS) $\rho\overline{u_iu_j}$. And the equation of volume fraction transport [17]:

$$\frac{\partial c}{\partial t}+\frac{\partial(cU_j)}{\partial x_j}=0 \quad (10)$$

c; volume fraction $=\frac{V_{air}}{V_{total}}$, ρ; fluid density and μ; viscosity is calculated as:

$$\mu=\mu_{air}c+\mu_{water}(1-c) \quad (11)$$

$$\rho=\rho_{air}c+\rho_{water}(1-c) \quad (12)$$

The turbulence model wall laws have restrictions on the y+ value at the wall. The wall y^+, a non-dimensional distance from the wall to the first grid point was similar to local Reynolds number represented in Equation 13. It's determining whether the influences in the wall-adjacent cells are laminar or turbulent. Turbulence models deal with the flow in the boundary layer can be further subdivided into a laminar (viscous) sublayer and a fully turbulent region.

$$y^+=\frac{U_\tau y}{\nu} \quad (13)$$

where, Uτ; frictional velocity as comparison between shear stress at the wall (τ_w) and density (ρ), y; distance from wall surface, ν; kinematic viscosity. The value y^+ of hull form was depending the wall surface adjusting to the flow in the boundary layer.

2.2. Last Experimental Result

The results of the experimental data by [18] was used to validate the CFD analysis on Wigley pentamaran hull form with asymmetric inner side-hulls. The experiment had done to 9 configurations at variations Fr 0.1 - 0.7. On model IIA with configuration S/L (separation/ length of main hull) 3/16

and R/L (stagger/ length of main hull) 1/ 20 at Fr 0.35 the resistance was reduced by 25%. At Froude numbers ranging from 0.2 to 0.7, the resistance coefficients have a downwards trend as shown in figure 1.

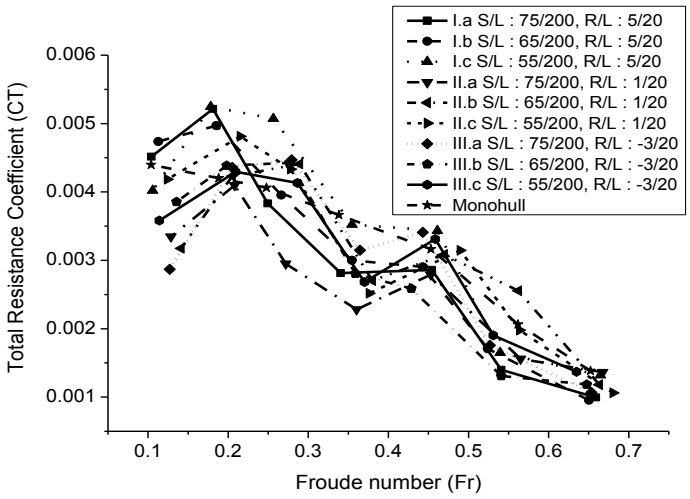

Figure 1. Total resistance coefficient [18]

Table 1. Model hull specification

Main Dimension	Wigley			Chine 25^0		
	Main	Inner side	Outer side	Main	Inner side	Outer side
LOA	2.00 m	1.00 m	0.75 m	2.40 m	1.02 m	0.93 m
B	0.20 m	0.10 m	0.07 m	0.20 m	0.10 m	0.07 m
T	0.07 m	0.07 m	0.06 m	0.07 m	0.07 m	0.06 m
H	0.15 m	0.15 m	0.14 m	0.15 m	0.15 m	0.14 m
Cb	0.57	0.59	0.58	0.59	0.67	0.55
WSA	0.39 m^2	0.18 m^2	0.11 m^2	0.55 m^2	0.30 m^2	0.21 m^2
Δtot		24.5 kg			≈24.5 kg	
Main Dimension	Chine 30^0			Chine 35^0		
	Main	Inner side	Outer side	Main	Inner side	Outer side
LOA	2.75	1.08 m	0.93 m	3.30 m	1.12 m	0.93 m
B	0.20 m	0.10 m	0.07 m	0.20 m	0.10 m	0.07 m
T	0.07 m	0.07 m	0.06 m	0.07 m	0.07 m	0.06 m
H	0.15 m	0.15 m	0.4 m	0.15 m	0,15 m	0.14 m
Cb	0.52	0.65	0.55	0.44	0.62	0.55
WSA	0.61 m^2	0.31 m^2	0.21 m^2	0.69 m^2	0.32 m^2	0.21 m^2
Δtot		≈24.5 kg			≈24.5 kg	

The results of IIa configuration as initial modelling then performed with pentaraman chine hull form at variation of deadrise angles: 25^o, 30^o, 35^o. The first step was modelling an initial pentamaran which used Wigley linesplan of Yanuar experimental. The second, modified the Wigley hull form with chine form in the same S/L position. The specifications of both hull form was shown in table 1. Midship section of Wigley pentamaran and chine hull forms were designed as shown in figure 2 and 3. Transformation Wigley to chine form with some differences main hull L/B: 12; 13.75; 16.5 in constant B/T: 2.9 and H/T: 2.1, there are 6 new configurations from the initial configuration. In each deadrise

angle of chine hull form there are two configurations as shown in figure 4. Each configuration at each chine hull form is a change in the position of inner and outer side hull from its original position.

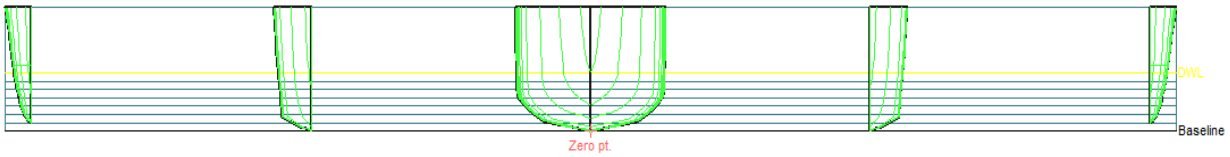

Figure 2. Pentamaran Wigley

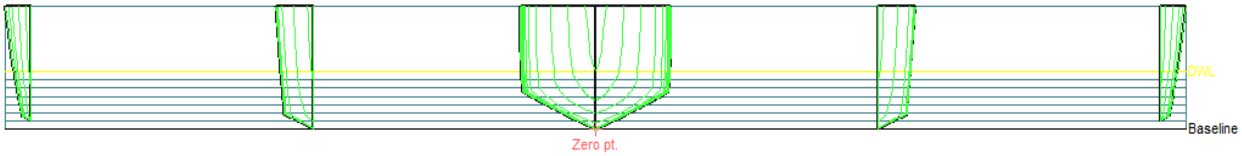

Figure 3. Pentamaran chine

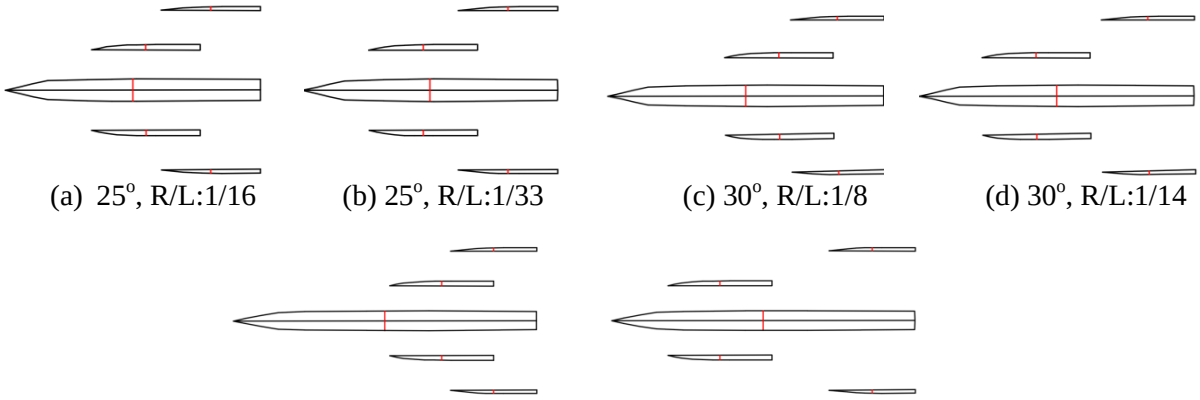

Figure 4. Six new configurations of chine hull form

2.3. Meshing Technique

Table 2. CFD simulation properties

Property	Fine Mesh
Type of mesh	Tetrahedral, mixer
Domain Physics	Homogeneous water/air multiphase, *K*-ε, automatic wall function, buoyancy model –density difference, standard free surface model
Boundary physics:	
Inlet	Inlet, volume fraction, turbulence intensity 0.05
Outlet	Outlet, relative pressure
side wall	Wall, free slip condition
Top	Opening, relative pressure 0 Pa
Hull/ Bottom	Wall, no slip condition
Symmetry plane	Along centerline of the hull
Solver settings:	
Convergence criteria	Residuary type: RMS, Target: 10-e4
Multiphase control	Volume fraction coupling

[19] and [17] revealed that mesh quality is very important to perform a reliable CFD. Total element number in the mesh should be large enough to represent the geometry and flow phenomena in the domain. Physical domains at free surface model for domain boundaries in detailed are provided in table 2. The mesh settings for element size was repeated 5 times (4.5M, 7M, 9M, 10M and 11M) to evaluate convergence. For verification, i.e. convergence and the assessment of numerical uncertainty, processing mesh has been carried out to the total resistance (force) which element size of boundary 0.1 and the hull of 0.005 to 0.003. The meshing results on the model shown in figure 5, which produced about 10 million elements. ICEM meshing method was selected to produce the mesh automatically. The mesh generated in ICEM using a low transition options to refine the mesh gradually. Unstructured tetrahedral elements were selected in the entire domain and hull.

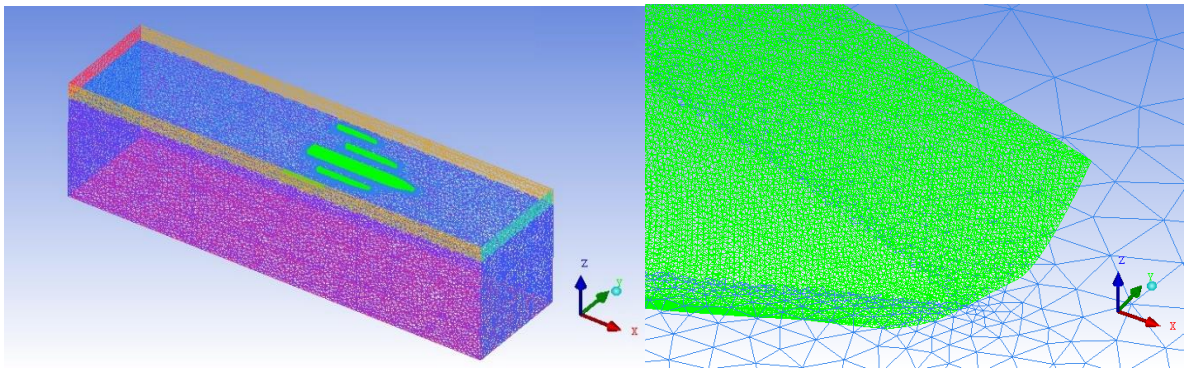

(a) Meshing domain (b) Hull meshing detail

Figure 5. CFD mesh analysis results

Total number of elements, mesh size as well as value of Y^+ was considered for several variations of mesh. The initial mesh created 4.5M elements then increased until to 11M elements with Y^+ on the hull ~5. In multiphase flow, volume fraction is considered to prevent a large residual. Repeated convergence was assumed through normal residuals. The residual RMS of domain required on 1E -04. The control time step for steady state problems, CFX uses a robust implicit formulation allowing the large time step can be determined, and accelerate convergence. Time step permits fixed time step size used for the entire flow domain. The flow was dominated by advection (horizontal mass movement which resulted in the change) the size of the time step should be scale length divided by the speed scale [20]. A steady state calculation usually requires between fifty to a hundred-time steps to achieve convergence. But overall a great time step makes an unstable convergence, otherwise if time step too small would be very slow convergence.

3. Results and Discussion

Transformation Wigley pentamaran into chine hull form on constant displacement causes the change of Lwl so the domain changed, particularly, the stern and bow hull forms adjust to the ship length. In addition to domain size, mesh settings and CFD setup follow the previously described arrangement, i.e.: mesh size, boundary conditions, time step and convergence controls. From the results of the CFD analysis and comparison with experimental data was shown in figure 6, which both graphs of total resistance coefficient (C_T) show similar trend. The difference between the experimental result and CFD was obtained by the equation (14). The difference average result of the cases was 3.6%, which shows CFD setup well-defined.

$$\Delta C_T = \frac{C_{T.exp} - C_{T.CFD}}{C_{T.exp}} x100\% \quad (14)$$

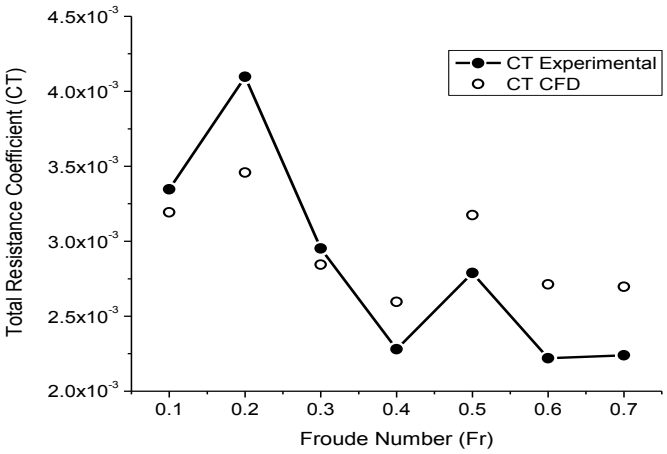

Figure 6. Comparison of C_T between experimental and CFD of Wigley hull form

The resistance coefficient results of 6 chine hull forms C_T, C_F and C_R were shown in figure 7 – 9, respectively. The results of C_T showed the smallest value was generated from chine 35^0 R/L:1/14 and R/L:1/7 with similar trend. The highest average of all chine hull form for C_T occur in 0.2-0.4 Fn. Then, by increase of Fr the C_T values gradually began to fall. At deadrise angle 35^0, it significantly has the smallest C_T compared to deadrise 25^0 and 30^0. It indicates that increased deadrise angle caused decrease the C_T value. The average reduction of C_T value as shown in figure 7 with chine 30^0 to 35^0 was about 9.75%, 25^0 to 30^0 was about 2.9%, and 25^0 to 35^0 was about 12.3%. The frictional resistance acting on a hull form for experimental refers to equation 4, while in CFX-Post could be calculated by performing an area integral of the wall shear in the x-direction. In figure 9 shows C_F graph has similar trend to C_T, where the lowest C_F value generated by chine 35^0 as well. While the greatest value of residual resistance (C_R) was shown by chine hull form 35^0 at R/L: 1/14 and R/L: 1/7. It means this model has bigger wave resistance component than the other forms.

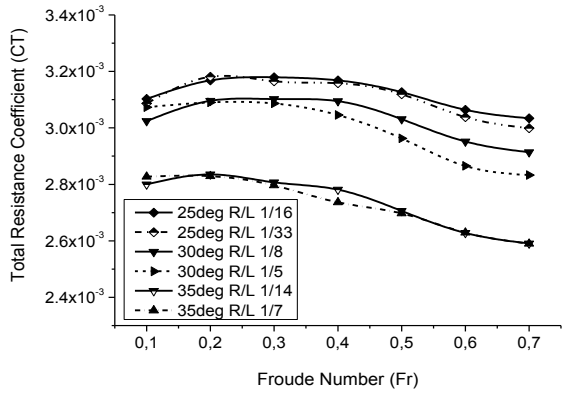

Figure 7. Result on total resistance coefficient (C_T)

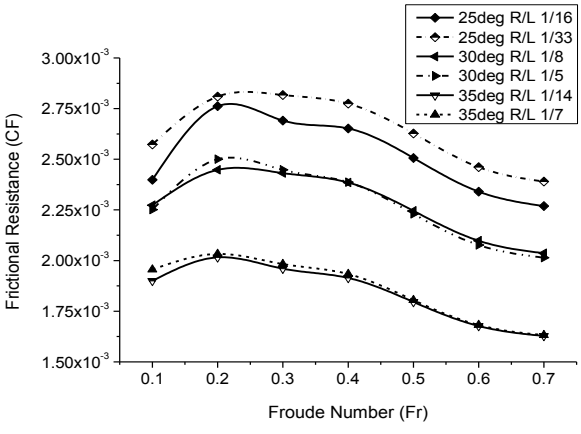

Figure 8. Result on friction coefficient (C_F)

The C_T graph of Wigley hull form appeared hump and hollow phenomenon, while the chine hull form there is no significantly increase or decrease of C_T in Fr variation. The drag reduction of Wigley pentamaran to chine hull form was represented by the equation (15). Percentage of drag reduction (D_R) results of 6 chine hull forms was shown in figure 10. While the maximum drag reduction successively to chine form set out in table 3.

$$DR(\%) = \left| \frac{CT_{wigley} - CT_{chine}}{CT_{wigley}} \right| \quad (15)$$

Table 3. Maximum drag reduction of chine hull form

chine	25deg R/L 1/16	25deg R/L 1/33	30deg R/L 1/8	30deg R/L 1/5	35deg R/L 1/14	35deg R/L 1/7
DR (%)	15,81	15,55	13,80	10,65	20,21	20,38

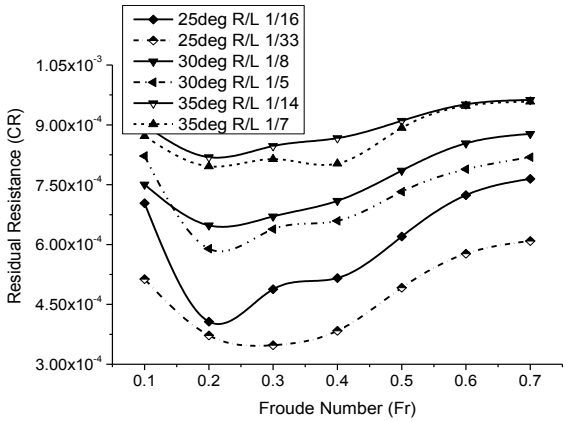

Figure 9. Result on residual resist. coeff. (C_R)

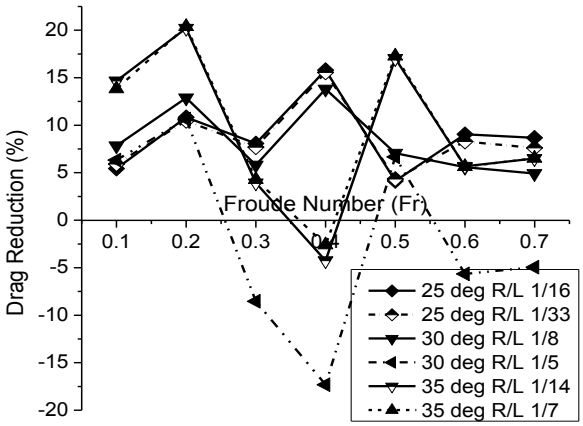

Figure 10. Percentage of drag reduction (D_R)

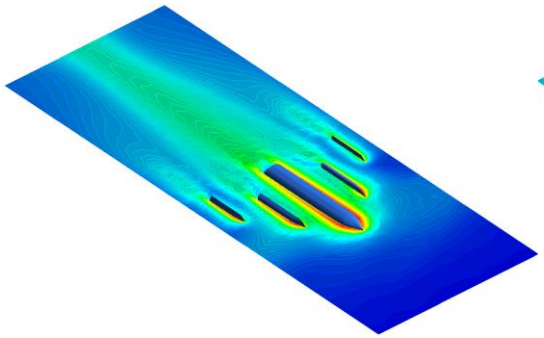

(a) Wigley Contours on z/Lpp = 0.035

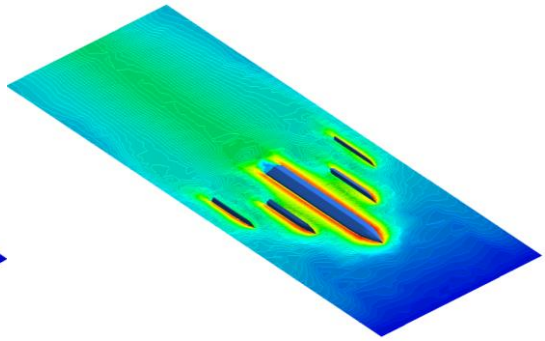

(b) Chine 25^0 Contours on z/Lpp = 0.03

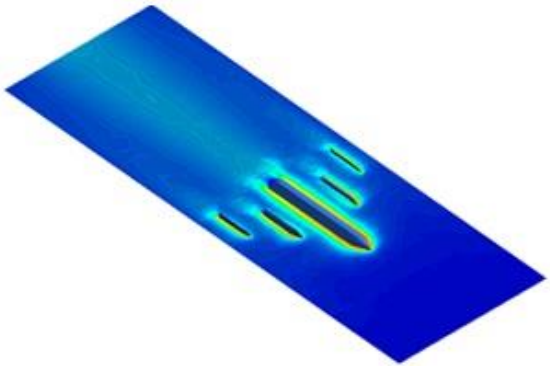

(c) Chine 30^0 Contours on z/Lpp = 0.025

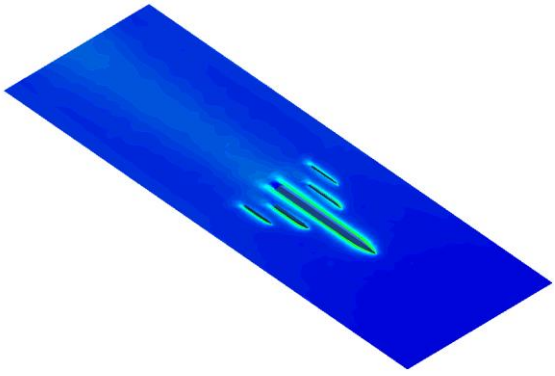

(d) Chine 35^0 Contours on z/Lpp = 0.02

Figure 11. Free surface elevation (reverse side), z/Lpp, of global wave pattern, Fn = 0.7

The contour of wave volume fraction from CFD simulation at Fr 0.7 for Wigley and chine forms were shown in figure 11. There are differences contour of wave volume fraction for Wigley and each chine, which blue colour (a) and (b) shows bigger wave than the dark blue, (c) and (d). It seems that the hull form of Wigley generates bigger wave effect than chine.

4. Conclusion

The comparison of CFD analysis between Wigley to chine form with inner and outer asymmetric hull showed the effect of increasing deadrise angle can improve drag reduction. The highest drag reduction of chine 35^0 due to the big deadrise angle would be causing unconstructed waves angle between each hull. Some advantages chine hull form compared to Wigley are:

- C_T value tends to be smaller on higher L/B with constant B/T and H/T;
- Increasing C_T value not fluctuate with increasing Fr;
- The greater deadrise made the smaller C_T;
- Drug reduction could reach 20.38 % at the largest angle 35^0 on Fr 0.2.

The implication for further research acknowledged needs to investigate the effect of the angle of entrance and stem angle of hull form to the resistance characteristic.

5. Acknowledgement

This work has been financially supported by Directorate of Research and Community Services, Universitas Indonesia (Hibah Ristek Dikti 2017). The authors would like to acknowledge the support of pentamaran team of Department of Mechanical Engineering.

6. References

[1] Oller, Erik, Vasilios Nikou, and Konstantinos Psallidas 2003 Focused Mission High Speed Combatant *DTIC Doc.*
[2] Yanuar, Ibadurrahman, Kurniawan T Waskito, S Karim, and M Ichsan 2017 Interference Resistance of Pentamaran Ship Model with Asymmetric Outrigger Configuration *J. of Marine Sci. and Appl.* **16**:42-47
[3] Ikeda, Yoshiho, Emiko Nakabayashi, and Ai Ito 2005 Concept design of a pentamaran type fast RoRo ship *J. of the Japan Soc. of Nav. Archit. and Oc. Eng* **1**:35-42
[4] Yanuar, Gunawan, Sunaryo, and A Jamaluddin 2012 Micro-bubble drag reduction on a high-speed vessel model *J. of Mar. Sci. and Appl.* Vol **11** Issue 3 Pages 301-304
[5] Chengyi, and Wang 1994 Resistance charicteristic of high-speed catamaran and its application *Shipbld. of China* **3**:003
[6] Blount, Donald L 1995 Factors Influencing the Selection of a Hard Chine or Round-Bilge Hull for High Froude Numbers *FAST '95* Travemunde Germany
[7] Moraes, HB, JM Vasconcellos, and RG Latorre 2004 Wave resistance for high-speed catamarans *Oc. Eng.* **31**(17):2253-2282
[8] Begovic, E, et al 2004 Pentamaran hull for medium size fast ferries *Hydrodynamics VI* (Eds L Cheng and K Yeow):**23-28**
[9] Bari, Ghazi S, and Konstantin I Matveev 2016 Hydrodynamic modeling of planing catamarans with symmetric hulls *Oc. Eng.* **115**:60-66
[10] Tarafder, Md Shahjada, Mir Tareque Ali, and Md Shahriar Nizam 2013 Numerical prediction of wave-making resistance of pentamaran in unbounded water using a surface panel method *Proc. Eng.* **56**:287-296
[11] Hsiung CC and Xu H 1988 Determining Optimal Forms of a Catamaran for Minimum Resistance by the Mathematical Programming *Meth.' Schiffstech* Bd **35**
[12] Peng 2001 Numerical computation of multi-hull ship resistance and motion *Dalhousie Univ. Halifax* Canada

[13] Michell JH 1898 The Wave-Resistance of a Ship *Phil. Magazine* Series **5** Vol 45 Xo 272 London January pp 105-1 23
[14] Menter FR 1994 Two-equation eddy-viscosity turbulence models for engineering applications *AIAA J.* **32**(8):1598 –605
[15] Versteeg, Henk Kaarle Malalasekera, Weeratunge 2007 An introduction to Computational Fluid Dynamics *The Finite Vol. Meth.* Pearson
[16] Wilcox DC 2006 Turbulence Modelling for CFD *3rd Ed. DCW Industr.*
[17] Ferziger JH and Peric M 2002 Computational Methods for Fluid Dynamics *3rd ed. Spring. Verlag* pp **157–206**
[18] Yanuar, Gunawan, Kurniawan T and A Jamaluddin 2015 Experimental Study Resistances of Asymmetrical Pentamaran Model with Separation and Staggered Hull Variation of Inner Side-Hulls *Inter. J. of Fluid Mech. Research* Vol **42** No 1
[19] Blazek J 2001 Computational Fluid Dynamics: Principles and Applications *Elsev. Sci. Ltd* Oxford England
[20] Seo JW, Seol DM, Lee JH and Rhee SH 2010 Flexible CFD meshing strategy for prediction of ship resistance and propulsion performance *Inter J. Nav. Arch. Oc. Eng*. **2** pp 139-14